

## FIB-SEM and TEMT Observation of Highly Elastic Rubbery Material with Nanomatrix Structure

Seiichi Kawahara,<sup>\*,†</sup> Yoshimasa Yamamoto,<sup>†</sup> Shuji Fujii,<sup>†</sup> Yoshinobu Isono,<sup>†</sup> Ken-ichi Niihara,<sup>‡</sup> Hiroshi Jinnai,<sup>‡</sup> Hideo Nishioka,<sup>§</sup> and Akio Takaoka<sup>||</sup>

Department of Materials Science and Technology, Faculty of Engineering, Nagaoka University of Technology, Nagaoka, Niigata 940-2188, Japan, Department of Macromolecular Science and Engineering, Graduate School of Science and Engineering, Kyoto Institute of Technology, Matsugasaki, Kyoto 606-8585, Japan, JEOL Ltd., 1-2-3 Musashino, Akishima, Tokyo 196-8556, Japan, and Research Center for Ultra-High Voltage Electron Microscopy, Osaka University, 7-1 Mihogaoka, Ibaraki, Osaka 567-0047, Japan

Received December 22, 2007

Revised Manuscript Received March 24, 2008

### Introduction

Recent research works on a morphology-control in nanometric scale with block- and graft-copolymers revealed a limitation of alignment of microphase separated structure, due to a grain boundary of ordinary cylinder, gyroid, and lamellar structures.<sup>1–6</sup> Thus, we have proposed a nanomatrix structure<sup>7</sup> to solve the unavoidable problem of the block- and graft-copolymers, i.e. the grain boundary.

The nanomatrix structure may be formed by covering particles with a nanolayer followed by coagulation of the resulting nanolayer-covered particles. In this case, the particles are required to chemically link to the nanolayer, in order to stabilize the nanomatrix-structure in equilibrium state. In particular, for the polymeric materials, the chemical linkages may be formed by graft-copolymerization of a monomer onto polymer particles in the latex stage, since the particles in the latex are dispersed in water. In the previous works,<sup>7,8</sup> in fact, we reported high grafting efficiency and high conversion of the graft-copolymerization of styrene onto natural rubber particle purified by deproteinization.<sup>9,10</sup> After the coagulation of the grafted natural rubber, we obtained an apparent two-dimensional image for the product through transmission electron microscopy, TEM. In the TEM image, the nanomatrix seemed to be smoothly connected to form a continuous phase.<sup>7</sup>

Recently, a serious problem on TEM images was, however, suggested by Jinnai and co-workers, on the basis of computer simulation and observation of the phase separated structure of a block-copolymer through transmission electron microtomography, TEMT.<sup>11</sup> The transmitted electron beam throughout an ultrathin section made an apparent two-dimensional image, different from a real object, because of a thickness of the section.<sup>12,13</sup> In other words, the TEM image is just a projection of three-dimensional entity; hence, structural information along a beam-through direction, perpendicular to the plane of the

specimen, i.e., the Z-direction, may be lost. To obtain the real image of the phase separated structure, therefore, we must perform the three-dimensional observation for the nanomatrix structure. The three-dimensional image is made by stacking tomograms reconstructed from a series of tilted transmitted two-dimensional images, which are taken by TEM. Although a resolution along the Z-direction is known to be less than that in the specimen plane, we may recognize the real structure through the Z-direction.

Furthermore, we have to take a notice of a diameter of the dispersoid of the nanomatrix structure, which is about a micrometer in diameter. Since the thickness of the ultrathin section is less than several hundred nanometers, the three-dimensional image is not obtained for the nanomatrix structure as long as we adapt TEMT; that is, the TEMT image is similar to the two-dimensional TEM image. To observe the nanomatrix structure in a range of nanometric scale and micrometric scale, we thus have to apply not only TEMT but also the recently proposed dual beam electron microscopy, i.e., field-emission scanning electron microscopy equipped with focused ion beam, FIB-SEM.<sup>11,14,15</sup> Using these techniques, we shall investigate a relationship between the properties and three-dimensional structure for the nanomatrix-structured material.

In the present work, we investigate a relationship between viscoelastic properties and morphology of the nanomatrix-structured material in comparison with that of the island-matrix-structured material, in which the nanomatrix structure and the island-matrix structure are formed by graft-copolymerization of styrene onto natural rubber. To form the nanomatrix structure, styrene is fed into natural rubber latex after adding an initiator.<sup>7,8</sup> Almost all polystyrene of about 10<sup>4</sup> g/mol in number average molecular weight,  $M_n$ , is chemically attached to natural rubber ( $M_n$ : ca. 3 × 10<sup>5</sup> g/mol) particle at the interface, as is evident from high grafting efficiency of styrene, i.e. more than 90 mol %, which was estimated from amount of polystyrene in the product before and after extraction with acetone/2-butanone 3:1 mixture.<sup>7,8</sup> In contrast, to form the island-matrix structure, the initiator is added after mixing natural rubber latex with styrene for more than an hour, in which the grafting efficiency of styrene is about 60 mol % and the molecular weight of the resulting polystyrene is about 10<sup>4</sup> g/mol.<sup>16</sup> The three-dimensional observation is performed for film specimen of the rubbers by FIB-SEM and TEMT.

### Experimental Section

Natural rubber latex used in the present study was commercial high-ammonia natural rubber latex. The incubation of the latex was made with 0.1 wt % (w/w) urea in the presence of 1 wt % sodium dodecyl sulfate (SDS) at 303 K followed by centrifugation at 10 000 rpm. The cloudy fraction was redispersed in 1 wt % SDS to make latex of 30 wt % in dry rubber content (DRC) and it was washed twice by centrifugation to prepare deproteinized natural rubber (DPNR) latex.<sup>9,10</sup> The DPNR latex was diluted with distilled water to adjust 10 wt % DRC, and the concentration of SDS was adjusted to 0.1 wt %.

Graft-copolymerization of styrene onto DPNR was carried out in latex stage with *tert*-butyl hydroperoxide/tetraethylene pentamine as an initiator. The DPNR latex was charged with N<sub>2</sub> gas for 1 h at 30 °C. The initiator of 3.3 × 10<sup>−2</sup> mol/kg of rubber and styrene of 1.5 mol/kg of rubber were added to the latex, respectively. The reaction was performed by stirring the latex at about 400 rpm for 2 h at 30 °C. The unreacted styrene was removed by using a rotary

\* To whom correspondence should be addressed at the Department of Materials Science and Technology, Faculty of Engineering, Nagaoka University of Technology, Nagaoka, Niigata 940-2188, Japan. Telephone: 81-258-47-9301. Fax: 81-258-47-9300. E-mail: kawahara@mst.nagaokaut.ac.jp.

<sup>†</sup> Department of Materials Science and Technology, Faculty of Engineering, Nagaoka University of Technology.

<sup>‡</sup> Department of Macromolecular Science and Engineering, Graduate School of Science and Engineering, Kyoto Institute of Technology.

<sup>§</sup> JEOL Ltd.

<sup>||</sup> Research Center for Ultra-High Voltage Electron Microscopy, Osaka University.

evaporator under reduced pressure. A film specimen of the grafted natural rubber was prepared by casting water from the reacted latex in a Petri dish, and it was dried under reduced pressure at ambient temperature for more than a week.<sup>7,8</sup>

Three-dimensional observation of the nanomatrix structure was carried out with a transmission electron microscope (TEM), JEOL JEM-2100 at accelerating voltage of 200 kV and an ultrahigh voltage electron microscope at Osaka University operated at 3 MV.<sup>17</sup> The former was used to take three-dimensional images presented in Figures 5 and 6, while the latter was used in Figure 4. The ultrathin sections of the graft-copolymer used for the former observation were prepared by a Sovall Instruments MT6000 ultramicrotome at a temperature lower than glass transition temperature of natural rubber. The thin sections were stained with osmium tetroxide (OsO<sub>4</sub>) at room temperature over one or two nights. The sections with ca. 500 nm thick used for the latter observation were prepared and stained with ruthenium tetroxide (RuO<sub>4</sub>) in the similar way as described above. A special specimen holder that enables us to rotate the section up to 90° was used. The tilt angular range in the particular experiment was −59° to +63° with an increment of 1°, which was aligned and reconstructed according to the protocol described in ref 18.

A low magnification three-dimensional image was obtained with a FIB-SEM, SII SMI-3050SE, at accelerating voltage of 3 kV, in which positively charged Ga ion at about 50 pA was used for milling process. Field emission SEM images of the graft-copolymer were taken after slicing its surface at each 102 nm interval with Ga ion. The three-dimensional image with a pixel size of × 15 nm, Y19 nm and Z102 nm was made by stacking reconstructed two-dimensional SEM images. To increase the pixel size at the Z-direction as it looks good, the same six images were stacked, each in 102 nm intervals, so that the pixel size of the completed three-dimensional image was X = 15 nm, Y = 19 nm, and Z = 17 nm.

Dynamic mechanical properties were measured with a Rheometric Science ARES-4 at frequencies between 0.1 and 10 Hz and temperatures between 213 and 403 K. The samples used were the as-prepared film, and the film was annealed at 130 °C for an hour.

## Results and Discussion

A storage modulus at plateau region (plateau-modulus) versus frequency for natural rubber, the rubber with the nanomatrix structure and the rubber with the island-matrix structure is shown in Figure 1. The value of the plateau modulus of natural rubber was about 10<sup>5</sup> Pa, as in the case of that reported in the literature.<sup>19</sup> When the nanomatrix structure was formed in natural rubber, the plateau modulus of the rubber increased about 10 times as high as that of natural rubber. In contrast, the plateau modulus increased a little, about 1.3 times, when the island-matrix structure was formed in natural rubber. The 1.3 times increase in the plateau modulus is the same as an ideal increase of 1.3 times estimated from the moduli of natural rubber and polystyrene by the following expression<sup>20</sup>

$$\sigma = E\gamma$$

$$E = \left\{ \frac{1-\lambda}{E_{PS}} + \frac{\lambda}{\phi E_{NR} + (1-\phi)E_{PS}} \right\}^{-1} \quad (1)$$

where  $\lambda$  and  $\phi$  represent volume fractions of the fragments in series and parallel models, respectively, and  $E_i$  is a storage modulus of  $i$  component, that is,  $E_{NR} = 10^5$  Pa and  $E_{PS} = 10^9$  Pa. The large increase in the plateau-modulus is an advantage of the nanomatrix structure, compared to the island-matrix structure, in which a ratio of natural rubber to polystyrene is the same, that is, about 90:10. We find a further increase in the plateau-modulus of the rubber with nanomatrix structure after annealing it at 130 °C, above glass transition temperature of

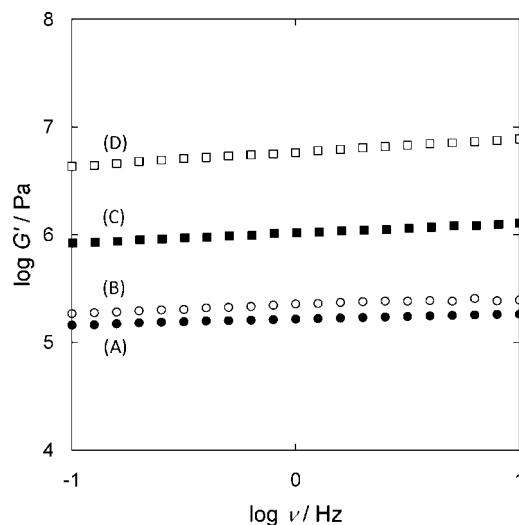


**Figure 1.** Storage modulus at plateau region versus frequency for (A) natural rubber, (B) DPNR-graft-PS (PS: ca. 10%) with island-matrix structure, (C) DPNR-graft-PS (PS: ca. 10%) with the nanomatrix structure annealed at 30 °C and (D) DPNR-graft-PS (PS: ca. 10%) with the nanomatrix structure annealed at 130 °C. The plateau modulus characteristic of the rubbery material increased a little with the island-matrix structure and dramatically with the nanomatrix structure, respectively. As for the nanomatrix-structured material, the plateau modulus increased about 35 times as high as that of natural rubber, after annealing it at 130 °C.

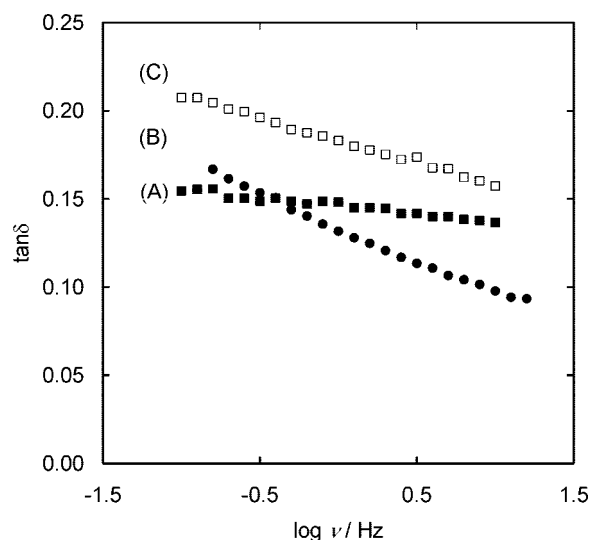


**Figure 2.** Loss tangent at plateau region versus frequency for (A) natural rubber, (B) DPNR-graft-PS (PS: ca. 10%) with the nanomatrix structure annealed at 30 °C and (C) DPNR-graft-PS (PS: ca. 10%) with the nanomatrix structure annealed at 130 °C. The loss tangent increased at high frequency region after forming the nanomatrix structure, and it increased significantly after annealing it at 130 °C.

polystyrene. The 35 times increase in the plateau modulus is a remarkable virtue characteristic of the nanomatrix structure.

Figure 2 shows a plot of loss tangent,  $\tan \delta$ , versus frequency at plateau region. The value of  $\tan \delta$  of natural rubber was in a region of 0.1 to 0.15, as in the case of literature value.<sup>19</sup> When we form the nanomatrix structure, the  $\tan \delta$  of the product increased dramatically at high frequency region but a little at low frequency region. After the product was annealed at 130 °C, the  $\tan \delta$  increased significantly over the entire frequency range at plateau region. This may be explained to be due to the well-connected nanomatrix at 130 °C but to the less-connected one at 30 °C. Thus, the product was proved to accomplish not only

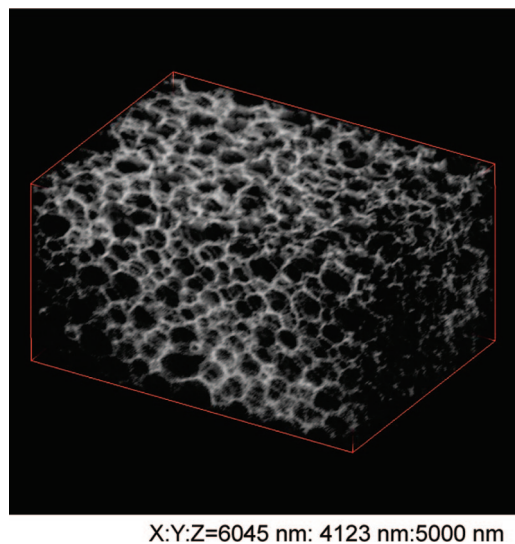


**Figure 3.** FIB-SEM image of the rubber with the nanomatrix structure before annealing. After aligning the observed surfaces sliced with the focused ion beam at each 7 nm interval, a three-dimensional image in micrometric scale was made for the rubber with the nanomatrix structure. The box size of the three-dimensional image is 6045 nm, 4123 nm, and 5000 nm in the *X*, *Y*, and *Z* directions, respectively.

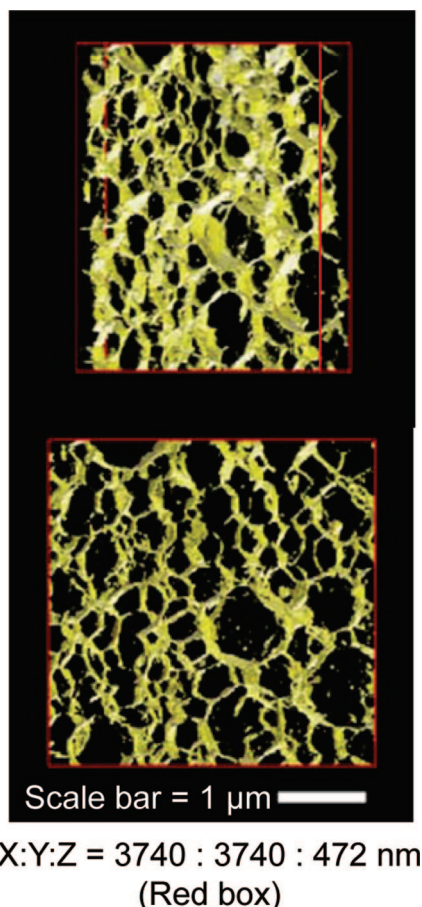


**Figure 4.** Three-dimensional TEMT image. To focus on the nanomatrix, the film was stained with  $\text{RuO}_4$  and the matrix was colored in the image; hence, transparent domains represent natural rubber and light yellow domains represent polystyrene. A mirror image indicates a three-dimensional picture. The scale bar shows 1  $\mu$ m. The box size of the three-dimensional image is 3740 nm, 3740 nm, and 472 nm in the *X*, *Y*, and *Z* directions, respectively.

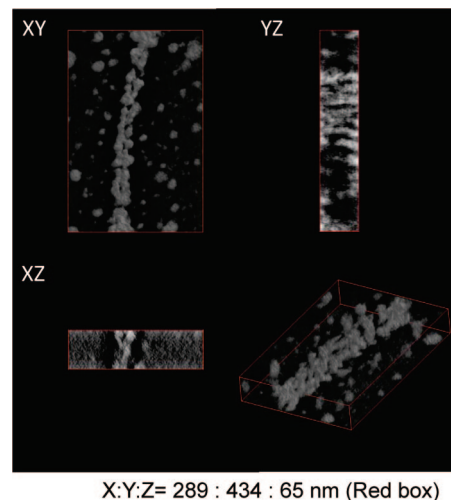


**Figure 5.** Orthogonal cross-sectional views and three-dimensional TEMT image of the rubber with the nanomatrix structure. The box size is 289 nm, 434 nm, and 65 nm, where the dark domains represent natural rubber and bright domains represent polystyrene. In a *XY* through view, the nanomatrix is confirmed to be about 15 nm in thickness, which is disconnected to each other in *XZ* and *YZ* edge views. The three-dimensional TEMT image reveals that a part of the matrix was connected to each other, whereas the other part was disconnected, before annealing.

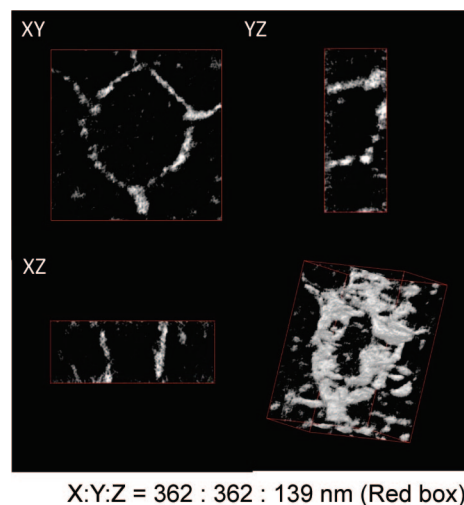


**Figure 6.** Orthogonal cross-sectional views and three-dimensional TEMT image of the rubber with the nanomatrix structure after annealing at 130  $^{\circ}\text{C}$ . The box size is 362 nm, 362 nm, and 139 nm, where dark domains represent natural rubber and bright domains represent polystyrene. In a *XY* through view, the nanomatrix of about 15 nm in thickness is shown to be connected each other. *XZ* and *YZ* edge views reveal that the thin nanomatrix is connected to each other after annealing. We may see the fused nanomatrix in the three-dimensional TEMT image.

high storage modulus but also outstanding loss modulus, where  $\tan \delta$  is a ratio of loss modulus to storage modulus. The difference in the storage modulus and loss tangent at the plateau region must come from a change in the morphology.

The FIB-SEM may give us a three-dimensional image of the nanomatrix-structure at low magnification; hence, we may recognize its entire image. After alignment of the observed images of surfaces, which were sliced with the focused ion beam at each 102 nm interval, a three-dimensional image was made for the nanomatrix structure (Figure 3). Since the surfaces were completely flat, without damage or void, we successfully constructed the three-dimensional image of the nanomatrix



structure in micrometric scale. At this low magnification, the bright polystyrene matrix was found to connect to each other in all directions. The natural rubber particles were positively confirmed to be dispersed into the nanomatrix of polystyrene.

TEMT observation at high magnification makes possible to investigate the matrix precisely. The three-dimensional TEMT image is shown in Figure 4. A curvature of the natural rubber particles was well-shown in the image, in spite of a limitation of thickness of the ultra thin section, i.e., about 100 nm. The natural rubber particles of various dimensions were randomly dispersed in the polystyrene matrix, reflecting a broad distribution of the particle dimension, i.e., from 50 nm to 3  $\mu\text{m}$  in volume mean particle diameter.<sup>21</sup> The three-dimensional image reveals not only the connected matrix but also its defect, at which rubber particles are fused to each other.

In order to focus on the defect to understand a reason why the dramatic increase in the plateau modulus occurs after annealing the rubber with the nanomatrix structure, we made the three-dimensional image of the nanomatrix at extremely high magnification. Figure 5 and Figure 6 show the three-dimensional TEMT images of nanomatrix structure before and after annealing the rubber with nanomatrix structure at 130 °C, respectively. The image of a through view in Figure 5 apparently showed the connected nanomatrix before annealing. However, the edge views revealed that a part of the nanomatrix was disconnected; that is, many lumps of granular polystyrene gathered to form the nanomatrix structure. A distance between the polystyrene granules was less than several nm, suggesting a flocculation of the granules. In contrast, after annealing, the granules were partly fused to each other (Figure 6). Thus, annealing may bring about the connected nanomatrix.

Based upon the three-dimensional observation at low and extremely high magnifications, the 10 times increase in the storage modulus may be associated with the flocculation of the polystyrene-granules to form the nanomatrix structure, which is distinguished from the isolated dispersoid in the island-matrix structure. The less than several nanometric spaces between the granules in the nanomatrix enable them to interfere to increase the storage modulus. The further increase in the plateau-modulus, i.e. 35 times, may be explained to be due to the connected nanomatrix after annealing. In an ordinary circumstance, the minor hard-component in the multicomponent system, consisting of hard and soft components, is known to become the island phase in the island-matrix structure for polymer blends or block- and graft-copolymers. In this case, little increase in the modulus is anticipated for the multi component systems. In contrast, it is difficult to form cocontinuous structures for the natural rubber/polystyrene 90:10 blend, taking account of their  $M_n$ . Only by forming the nanomatrix of

the minor component will we create tough, functional materials, which we have never seen.

In conclusion, the "nano-matrix structure" was proven to be a suitable structure to improve the viscoelastic property of rubbery material.

**Acknowledgment.** This work was supported in part by a Grant-in-Aid (12416) for the Development of Innovation and the 21st Century COE Program for Scientific Research from The ministry of Education, Science and Culture Japan, and Grant-in-Aid (17550786) for Scientific Research (C) from the Japan Society for the Promotion of Science.

## References and Notes

- (1) Chen, H. L.; Lu, J. S.; Yu, C. H.; Yeh, C. L.; Jeng, U. S.; Chen, W. C. *Macromolecules* **2007**, *40*, 3271–3276.
- (2) Ly, D. Q.; Honda, T.; Kawakatsu, T.; Zvelindovsky, A. V. *Macromolecules* **2007**, *40*, 2928–2935.
- (3) Takeshita, H.; Fukumoto, K.; Ohnishi, T.; Ohkubo, T.; Miya, M.; Takenaka, K.; Shiomi, T. *Polymer* **2006**, *47*, 8210–8218.
- (4) Roland, C. M.; Trask, S. A. *Rubber Chem. Technol.* **1989**, *62*, 896–907.
- (5) Akiyama, S.; Kawahara, S. In *The Polymeric Materials Encyclopedia*; Joseph, C. S., Ed.; CRC Press: New York, 1996; pp 699–709.
- (6) Tinker, A. J.; Jones, K. P. *Blends of Natural Rubber*; Chapman & Hall: London, 1998.
- (7) Kawahara, S.; Kawazura, T.; Sawada, T.; Isono, Y. *Polymer* **2003**, *44*, 4527–4531.
- (8) Pukkate, N.; Kitai, T.; Yamamoto, Y.; Kawazura, T.; Sakdapipanich, J.; Kawahara, S. *Eur. Polym. J.* **2007**, *43*, 3208–3214.
- (9) Kawahara, S.; Klinklai, W.; Kuroda, H.; Isono, Y. *Polym. Adv. Technol.* **2004**, *15*, 181–184.
- (10) Klinklai, W.; Saito, T.; Kawahara, S.; Tashiro, K.; Suzuki, Y.; Sakdapipanich, J. T.; Isono, Y. *J. Appl. Polym. Sci.* **2004**, *93*, 555–559.
- (11) Kato, M.; Ito, T.; Aoyama, Y.; Sawa, K.; Kaneko, T.; Kawase, N.; Jinnai, H. *J. Polym. Sci. Part B: Polym. Phys.* **2007**, *45*, 677–683.
- (12) Kaneko, T.; Nishioka, H.; Nishi, T.; Jinnai, H. *J. Electron Microsc.* **2005**, *54*, 437–444.
- (13) Kawase, N.; Kato, M.; Nishioka, H.; Jinnai, H. *Ultramicroscopy* **2007**, *107*, 8–15.
- (14) Brostow, W.; Gorman, B. P.; Olea-Mejia, O. *Mater. Lett.* **2007**, *61*, 1333–1336.
- (15) Beach, E.; Keefe, M.; Heeschen, W.; Rothe, D. *Polymer* **2005**, *46*, 11195–11197.
- (16) Fukushima, Y.; Kawahara, S.; Tanaka, Y. *J. Rubber. Res.* **1998**, *1*, 154–166.
- (17) Takaoka, A.; Ura, K.; Mori, H.; Katsuta, T.; Matsui, I.; Hayashi, S. *J. Electron Microsc.* **1997**, *46*, 447–456.
- (18) Jinnai, H.; Nishikawa, Y.; Ikehara, T.; Nishi, T. *Adv. Polym. Sci.* **2004**, *170*, 115–167.
- (19) Roberts, A. D. *Natural Rubber Science and Technology*; Oxford University Press: Oxford, U.K., 1988.
- (20) Takayanagi, M.; Imada, K.; Kajiyama, T. *J. Polym. Sci., Polym. Symp.* **1996**, *15*, 263–281.
- (21) Kawahara, S.; Washino, K.; Morita, T.; Tanaka, Y.; Isono, Y. *Rubber Chem. Technol.* **2001**, *74*, 295–302.

MA7028538